IEEE Access
Multidisciplinary | Rapid Review | Open Access Journal

Date of publication xxxx 00, 0000, date of current version xxxx 00, 0000.

Digital Object Identifier 10.1109/ACCESS.2022.Doi Number

A Versatile Embedded Platform for Implementation of Biocooperative Control in Upper-Limb Neuromotor Rehabilitation Scenarios

Ana Cisnal[1], (Student Member, IEEE), Daniel Antolínez[1], Javier P. Turiel[1], Juan Carlos Fraile[1], and Eusebio de la Fuente[1]

[1]Instituto de las Tecnologías Avanzadas de la Producción (ITAP), University of Valladolid, 47011, Valladolid, Spain.

Corresponding author: Ana Cisnal (e-mail: cisnal@ieee.org).

This work was supported by the Ministry of Science and Innovation, through the research projects PID2019-111023RB-C33 and RTC2019-007350-1, by the company TICCYL Digital S.L.U and by the support of the Regional Ministry of Education for the predoctoral recruitment of research staff co-financed by the European Social Fund (ESF).

ABSTRACT Biocooperative control uses both biomechanical and physiological information of the user to achieve a reliable human-robot interaction. In the context of neuromotor rehabilitation, such control can enhance rehabilitation experience and outcomes. However, the high cost and large volume of the commercial systems for physiological signal acquisition are major limitations for the development of such control. We present a highly versatile, low-cost and wearable embedded system that integrates the most commonly used sensors in this field: inertial measurement unit (IMU), electrocardiography (ECG), electromyography (EMG), galvanic skin response (GSR) and skin temperature (SKT) sensors. Additionally, the compact system combines wireless communication for data transmission and a high-efficiency microcontroller for real-time signal processing and control. We tested the system in two common neuromotor rehabilitation scenarios. The first is an upper-limb rehabilitation VR-based exergame, in which the patient must collect as many coins as possible. Movement recognition of the hand and arm is performed based on EMG and IMU information, respectively. The second is adaptive assistive control that adjusts the level of assistance of a wrist rehabilitation robot according to the physiological state and motor performance of the patient using GSR, ECG and SKT data. The quality of the recorded signals and the processing capacity of the system meet the needs of the two upper-limb rehabilitation applications. The wearable system is highly versatile, open, configurable and low cost, and it could promote the development of real-time biocooperative control for a wide range of neuromotor rehabilitation applications.

INDEX TERMS Biocooperative control, embedded system, neuromotor rehabilitation, real-time signal processing, wearable sensors.

I. INTRODUCTION

The concept of bio-cooperative control emerged in the field of robotics, specifically in rehabilitation robotics, during the last years of the first decade of the 21st century. The first formal appearance of the term biocooperative came from R. Riener, who proposed the integration of a human into the control loop not only by using biomechanical information but also by considering psycho-physiological parameters [1], [2].

This "human-in-the-loop" integration, from a biomechanical viewpoint, is usually performed by integrating position and force sensors into a mechatronic device. It ensures safety and enables the human to influence the movement of the robot (user-cooperative). The inclusion of physiological-related or psychological information in the loop allows the determination of the physical effort and emotional state of the patient, so the robot assistance can be challenging while ensuring that not

stress or physical harm is caused, leading to an enhanced rehabilitation experience.

A current trend in the field of rehabilitation is the development of multimodal human-robot interfaces (HRIs) [3], which are able to fuse and interpret data captured by multiple sensors, either physiological or biomechanical or a combination of both. In this sense, an extended strategy to drive rehabilitation robots is to recognize the intention of the movement of the user. Zhang et al. developed a human–machine interface using electrooculography (EOG), electroencephalography (EEG) and electromyography (EMG) signals to control a soft robotic hand in real time [4]. EMG has also been used in combination with inertial measruement units (IMUs) [5], [6] or accelerometers [7] to control assistive devices.

Another strategy commonly used is implementation of an assist-as-needed (AAN) paradigm. It is commonly used since it has been shown to increase the efficacy of rehabilitation. It adjusts the level of assistance of the robot to the patient's condition: the robot assists the human with just the necessary force so that the patient can complete the desired movement. The level of robot assistance is automatically adjusted to the user's state by evaluating their performance through physiological and/or biomechanical information.

AAN controllers have been implemented using biomechanical information of the subject extracted from accelerometers [8] or force sensors [9]. The torque applied by the subject has also been estimated by analyzing EMG signals to adapt the level of assistance of a robot by implementing EMG-based AAN controls [10-12].

Scotto et al. [13] adapted the level of assistance of an end-effector upper-limb rehabilitation robot considering the patient's performance and fatigue. The level of patient performance was determined using the biomechanical information extracted from an IMU sensor, while the level of muscular fatigue was estimated using EMG signals. Novak et al. [14] adjusted the difficulty of an upper extremity rehabilitation task by using biomechanics (force and movement), task performance and multiple features extracted from physiological signals, such as electrocardiography (ECG), galvanic skin response (GSR), respiration (RESP) and skin temperature (SKT) signals.

Mihelj et al. [15] generated the next action primitives of an upper extremity rehabilitation device using a two-stage fuzzy logic model. The first stage calculated motor performance from position and force, arousal from RESP signal and GSR features, specifically the skin conductance level (SCL) and response (SCR), and valence from the RESP rate and SKT. The second stage selected the action primitives (e.g. next haptic stage, keep visual stage, previous acoustic stage) based on the physical effort associated with the motor performance, arousal and valence.

AAN control has also been implemented by only identifying physiological states, such as emotions, affective states, or level of stress, without considering biomechanical information. For example, Rodriguez-Guerrero et al. [16] modulated the assistance provided by a haptic controlled robot as a function of user emotions. Emotions were estimated considering the 3-dimensional emotion model (arousal, dominance, and valence) using the HR mean, SCL mean and SCR frequency as inputs of a fuzzy logic model.

Emotion recognition (pleasant, neutral, or unpleasant) was addressed using both gradient boosting machines (GBMs) and convolutional neural networks (CNNs) based on EEG, blood volume pulse (BVP), SKT and SCL recordings [17]. An emotion recognition model was also developed considering six basic emotions (anger, sadness, fear, disgust, happiness and surprise) using EEG, EMG, electrooculography (EOG), BVP, SCL and interbeat intervals (IBI) signals. A weighted linear fusion model was proposed, and different combinations of features and classification methods, such as support vector machine (SVM) and k-nearest neighbors (KNN), were tested, obtaining accuracies ranging from 65-82% [18]. Detection of basic emotions, considering two, three or four states (regret, rejoice, blended, and none), was also investigated using heart rate (HR) and SCL measurements. The study compared the emotion detection accuracy when implementing different classification and regression algorithms and using different sliding window lengths, obtaining a maximum accuracy of 67% for binary classification using the classification and regression trees (CART) algorithm [19].

Koelstra et al. [20] used EOG, four EMG signals, 32 EEG electrodes, and GSR, BVP, SKT and RESP data to map emotions in a two-dimensional model (arousal and valence). J. Kim et al. acquired EMG, SC, ECG and RESP signals for determining arousal and valence [21]. Mandryk et al. [22] also identified these two emotions using normalized GSR, HR and EMG signals as inputs to a fuzzy logic control scheme characterized by 22 rules

Liu et al. [23] developed a model for affection recognition considering three target affective states (anxiety, engagement and liking) with an accuracy rate of 69-82%. The SVM-based recognizer model used different features derived from electrocardiography (EEG), photoplethysmography (PPG), heart sound, bioimpedance, GSR, EMG and SKT signals. Picard et al. [24] used KNN to classify eight emotions using features extracted from EMG, GSR, RESP and BVP waveforms.

Differentiation of stress and normal states was carried out using SVM with an 80% accuracy using features derived from BVP, GSR and pupil diameter (PD) signals [25]. A classification method to detect three different levels of stress (relaxed, medium level and overstress) was developed using the pulse rate, the RESP rate, the SKT and SCL and SCR features of the GSR using different learning

algorithms with an accuracy of up to 91%. The detected level of stress was used to adaptively and dynamically modify the level of difficulty of an end-effector upper-limb robotic device and a virtual reality (VR) system [26]. The evolution of HRIs in this field is going toward using multimodal information, combining different sensors to acquire physiological and/or biomechanical data [27]. Although there is great diversity in the selection of physiological signals and their features in HRI studies, to estimate cognitive or emotional aspects, ECG, GSR, SKT and EMG signals are commonly used.

However, one of the main challenges of using physiological signals, in addition to the complexity of designing a reliable control loop, is the high cost and volume of the required acquisition systems. It is important to remark that only a very few studies have developed their own sensing platform [28], and the vast majority of previous works integrate costly and bulky commercial products such as the MP150 system (BIOPAC, CA, USA) [12], [16], [23], Neuroscan NuAmps Express system (Compumedics Ltd., Australia) [4], ActiveTwo system (Biosemi, Netherlands) [20] and ProComp/FlexComp Infiniti System (Thought Technology Ltd., Canada) [17], [18], [21], [22], [24].

An approach for minimizing the volume is to integrate the sensors into the system itself. Jakopin et al. [29] integrated an ECG sensor, a GSR sensor, an NTC thermistor (temperature sensor), a pulse sensor (PPG) and a force cell into the handle of an end-effector rehabilitation robot. Postolache et al. [30] embedded ECG and skin conductivity (SCK) measuring channels, an accelerometer and flexible force sensors on a wheelchair. Heuer et al. [31] proposed an in-vehicle physiological data acquisition system that integrated direct contact sensors on a steering wheel to measure ECG, GSR, SpO2 level and SKT signals. Ilius Faisal et al. [32] developed a wearable device to monitor and assess the knee joint and mobility, which integrated IMU, temperature, pressure and GSR sensors. However, this approach not only minimizes the volume but also reduces the flexibility.

Although the vast majority of analyzed works have been developed using costly and bulky commercial systems without any processing capabilities, emerging multimodal fusion strategies require wearable sensing devices with high computational power, a small size, and a low cost to detect human physical activity and emotions [33]. Considering the portability and comfort of sensor wearing, it is necessary to carefully choose the number of sensors so that the system can be fast, energy efficient and convenient. Furthermore, a small set of sensors with the proper location can enhance the user's acceptance [33].

For this reason, a compact embedded system that integrates different low-cost sensors for implementation of a wide range of neurorehabilitation training exercises is presented in this paper. The system includes IMU, ECG, EMG, GSR and SKT sensors, which are some of the most commonly used sensors in biocooperative systems but can also be embedded such that they can be worn as an armband so that they will be comfortable. The small-sized system is wearable and features Bluetooth technology for data transmission. Furthermore, the system is open and highly configurable and integrates a high computational performance microcontroller to enable developers to implement signal processing and control algorithms in real time without the need for additional computing systems.

II. METHODS

The proposed embedded sensor wearable device combines various sensors along with a high-efficiency real-time microcontroller (MCU) and wireless communication, providing high flexibility and processing capacities for implementing biocooperative controllers. The high-level block diagram is shown in Fig. 1. The device is battery powered and includes five sensors (IMU, ECG, EMG, GSR, and SKT), which are directly connected to a 32-bit TMS320F28069M MCU (Texas Instruments, TX, USA) for real-time data processing and control. The acquired and processed data can be transmitted by a Bluetooth low energy (BLE) MCU CC2650 (Texas Instruments, TX, USA). Temporary access to the MCUs is allowed using a JTAG connection. Snap-lead pre-gelled electrodes are used for recording biopotentials (EMG and ECG), and two finger electrodes allow GSR collection. For movement and SKT measurements, the device must rest on the user.

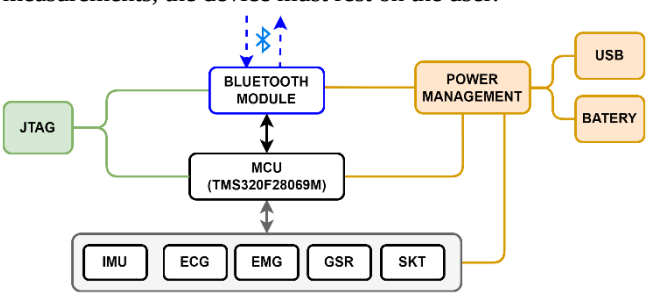

FIGURE 1. **Block diagram of the proposed embedded platform.**

A. SIGNAL ACQUISITION FRONT-END

The main component that allows identifying user movements is an ICM-20948 9-axis MEMS motion tracking device (InvenSense, CA, USA). It consists of a 3-axis gyroscope, an accelerometer and a compass with programmable filters and sensitivities. It also incorporates a digital motion processor (DMP) that offloads computation of the motion processing algorithm from the TMS320F28069M, improving the system power performance. The ICM-20948 is powered at 1.8 V, and it interfaces with the TMS320F28069M via Fast Mode i2C.

ECG measurements can be performed with the fully integrated single-lead ECG front-end AD8232 (Analog Devices Inc., MA, USA). It amplifies and filters the ECG

signals, which are then analog-to-digital converted in the TMS320F28069M with 12-bit resolution. The AD8232 chip also includes an AC lead-off detection mode to check whether both electrodes are properly connected. Using two digital signals, the AD8232 indicates the status of the electrode connection. The AD8232 is powered by 3.3 V, and the electrodes are connected using a jack connector.

A 2-channel electromyographic data acquisition unit is integrated into the printed circuit board. The two differential EMG signals are amplified and filtered prior to sampling using the analog front-end (AFE) MCP3912 (Microchip Technology Inc., AZ, USA). Compensation of differential input offset has also been considered in the design. The MCP3912 analog-to-digital converter (ADC) is fully configurable and interfaces with the TMS320F28069M using SPI communication [34]. The GSR is measured by attaching two electrodes to two hand fingers. The GSR module uses a low constant voltage technique; an electrical potential is applied between two skin contact points, and the resulting current flow between them is measured. The module is mainly composed of an LM324 quadruple operational amplifier (Texas Instruments, TX, USA). The analog output, which is the amplified and filtered voltage difference of the two electrodes, is transmitted to the ADC of the TMS320F28069M.

The body temperature is measured by an MLX90614 infrared (IR) thermometer (Melexis, Belgium). The advantage of IR technology is that there is no need for physical contact; therefore, skin temperature can be easily continuously monitored. The MLX90614 integrates an IR-sensitive thermopile detector chip and a signal conditioning application-specific standard product, which counts with a low-noise amplifier, a 17-bit ADC and a digital signal processing unit, resulting in a measurement resolution of 0.02 °C. The thermometer is powered at 3.3 V and interfaces with the TMS320F28069M via i2C.

B. SYSTEM LEVEL DESIGN

The real-time TMS320F28069M MCU is responsible for data processing and interfacing with the sensors, and its Harvard architecture is optimized to perform real-time tasks. It has a high-efficiency 32-bit CPU that runs at up to 90 MHz, a floating-point unit and a programmable control law accelerator (CLA), which executes code independently from the main CPU. This MCU allows efficient processing of the acquired signals and implementation of the required algorithms. It is equipped with 100 KB of flash, 100 KB of RAM and 2 KB of one-time programmable ROM. It has a built-in 12-bit ADC allowing sampling up to 3.46 MSPS (mega samples per second), several serial port communication peripherals (SPI, i2C, UART...) and timers, which are used to interface with the other elements of the proposed wearable solution. This powerful MCU has been chosen to allow advanced onboard processing of the acquired data with a normal current consumption of 245 mA, although it allows low-power operating modes.

To obtain a wireless and wearable device, the CC2650 MCU was incorporated into the proposed system. This system-on-chip provides an ultralow power BLE solution using a 2.4 GHz RF transceiver. The device is built on an ARM® Cortex®-M3 processor that handles the application layer and BLE protocol stack and an autonomous radio core centered on an ARM Cortex®-M0 processor that handles all the low-level radio control and processing associated with the physical layer and parts of the link layer. This single-chip interfaces with the TMS320F28069M using serial communication (i2C, SPI or UART) and transmits the processed data to a central device. The printed circuit board (PCB) integrates a BLE antenna, which was designed based on the TI specifications and built on the top copper layer of the board. Hence, there is no need to externally add an antenna. The board integrates 11 pads to simply and independently access the JTAG ports of the two MCUs for debugging and programming purposes.

The device is powered by a rechargeable lithium ion polymer battery with a capacity of 3500 mAh at 3.7 V (68x55x7 mm). The battery life is approximately 5 hours, considering that the estimated total maximum power of the device is approximately 1250 mW. The battery is recharged from a USB-C port using an MCP73831 dedicated integrated circuit (Microchip Technology Inc., AZ, USA). It uses a constant current followed by a constant voltage charging method. While the battery is recharging, the circuit is still powered by a USB port. The linear charge management controller automatically detects if the battery is present and continuously monitors the voltage to recharge the battery if the voltage drops below the recharge threshold.

The 2-layer PCB has been designed to maximize the signal integrity. It has split power planes (separated analog and digital signals), and the trace width is 12 mils except for the traces of the power signals, which are 24 mils wide. SMD components are used to reduce the board size, placing 0402 (1005 metric) SMD passive components on it. All discrete components are placed on the top layer to reduce assembly costs, with the exception of the thermometer. Three holes are included in the board to attach it to a cover box. The layout of the components was designed considering the different submodules (Fig. 2.a), resulting in a board size of 63x83 mm.

In summary, a versatile compact wireless embedded solution has been designed. The system incorporates several sensors and the AFE necessary to acquire different signals (ECG, EMG, GSR, SKT and motion). The processing of the recorded signals can be carried out on either the TMS320F28069M or the CC2650 or by combining both

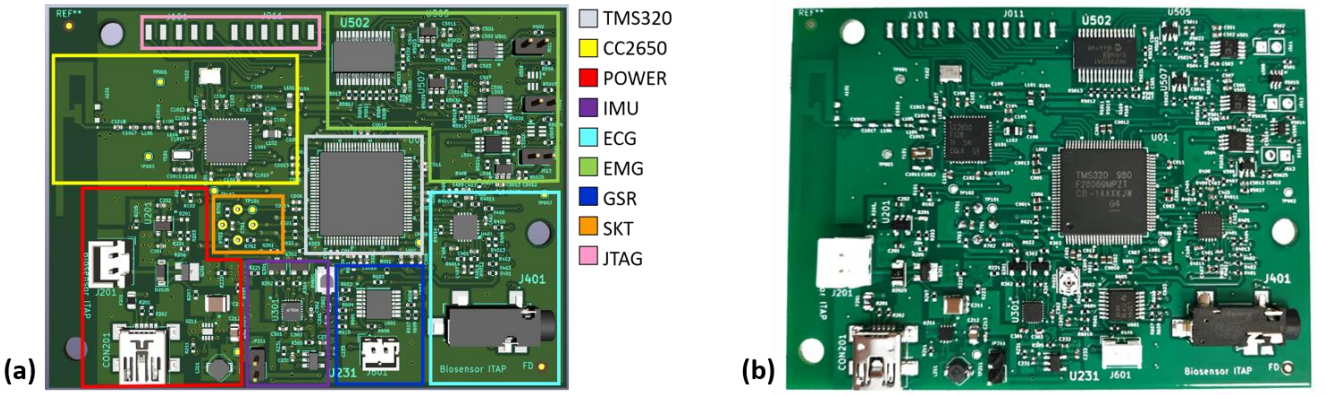

FIGURE 2. System design. (a) Layout of the components (b) Top view of the assembled PCB.

MCUs. The resulting data can be transmitted using BLE 4.1 to a central device. Furthermore, the developed solution has a relatively small size and a very low cost considering the large number of sensors and components (MCU; BLE communication, GSR, ECG, and EMG components; position sensor; thermometer; and power system). The final solution (Fig. 2.b) is housed in a 3D printed box and can be adjusted on the user arm using Velcro straps.

III. RESULTS

One of the requirements of the presented system is that it should be versatile so that it can be used in multiple applications in the field of neuromotor rehabilitation. In this section, two different rehabilitation scenarios are proposed. The first is based on the recognition of hand and arm movements using a VR-based exergame (Fig. 3.a). The second is an implementation of adaptive assistance control based on the emotional state and motor performance using a wrist rehabilitation robot (Fig. 3.b). Additionally, a detailed analysis of the system power consumption is carried out in this section.

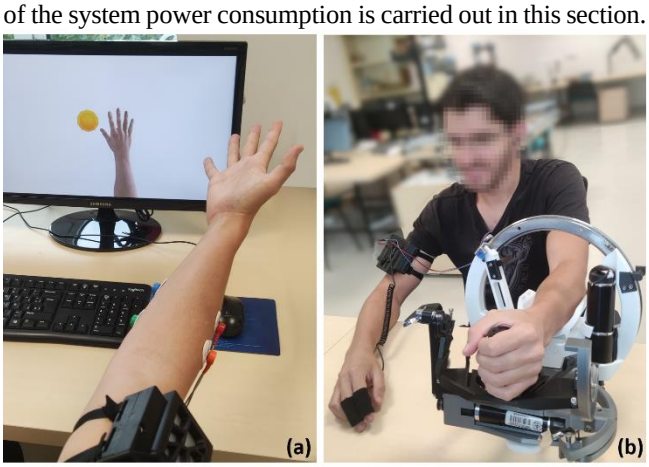

FIGURE 3. Proposed rehabilitation scenarios (a) Upper-limb rehabilitation using VR-based exergames (b) Rehabilitation setup for adaptive control using a wrist rehabilitation robot.

A. MOVEMENT RECOGNITION CONTROL

The first scenario is a VR-based exergame for upper-limb rehabilitation. The aim of the exergame is to collect as many coins as possible in a predefined time. For this purpose, the participant must move their arm and hand to interact with the environment. Specifically, to collect a coin, the user must move the arm to position the open or resting hand over the coin and then close the hand.

The exergame is designed to recognize arm and hand movements, allowing interaction with the target coins in the virtual environment. The arm orientation is computed from data measured by the ICM-20948, which is located on the user's arm. The hand gesture (open, rest or close) is determined from the EMG signals captured from the flexor digitorum superficialis (FDS) and extensor digitorum (ED) muscles, which are the muscles responsible for hand opening and closing. Arm orientation estimation and hand gesture recognition are performed in real time in the TMS320F28069M MCU and transmitted to the PC via BLE to update the VR scenario according to the estimated subject movements (Fig. 4). The VR scenario, which is mainly composed of a human arm and a coin, was designed in Unity and receives the processed data from the wearable system. Hence, the human arm orientation is updated using the estimated orientation, while the hand finger positions are updated according to the recognized gesture.

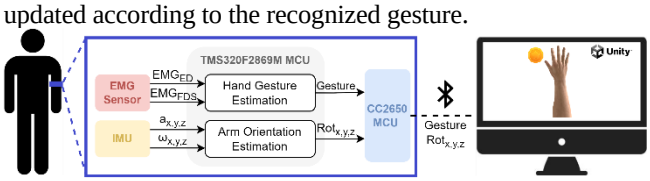

FIGURE 4. Integration of the proposed system with the virtual VR-based exergame for hand and arm rehabilitation.

Additionally, the exergame provides real-time adaptation of the difficulty to avoid frustration and maintain user motivation. The difficulty level is updated after collecting a coin and is based on the time spent collecting the last coin. The difficulty is modified by the degree of hand closure

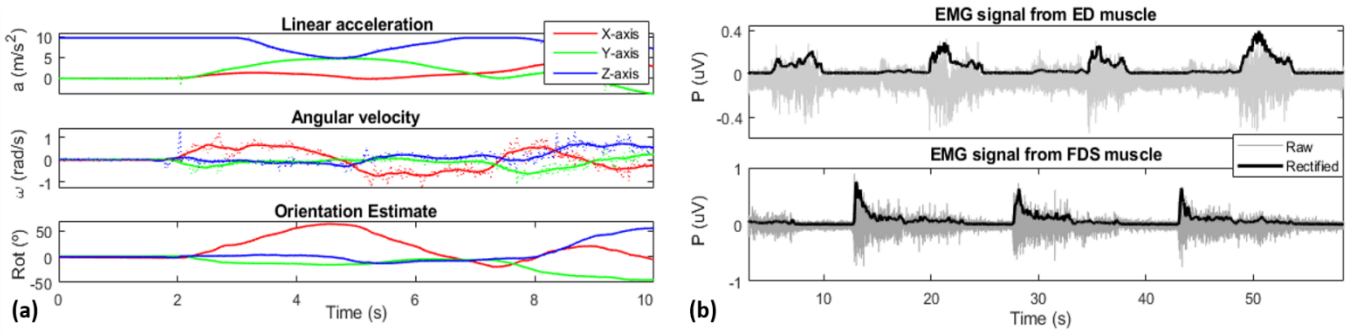

FIGURE 5. Signal processing for the proposed motion recognition control (a) Linear acceleration, angular velocity and estimated orientation (b) Raw EMG and rectified signals of ED and FDS muscles.

required to collect the coin and by the size and position relative to the current position of the new coin.

Fig. 3.a shows user rehabilitation with the VR-based exergame. The embedded platform is placed on the arm of the user, and two pairs of surface electrodes for recording the EMG signals are attached to the ED and FDS muscles, while the reference electrode is attached to the olecranon.

1) ACCELERATION AND GYROSCOPE READINGS

The ICM-20948 includes a 16-bit 3-axis gyroscope and an accelerometer. The gyroscope and accelerometer are configured to work with a full-scale range of ±250 dps (degrees per second) and ±2 g (19.6 m/s2), respectively. Hence, the ADC resolution is 131 LSB/dps and 16384 LSB/g. Linear acceleration and angular velocity are sampled at 100 Hz and transmitted to the MCU via 400 kHz Fast Mode i2C.

The orientation is estimated using a model whose inputs are the accelerometer and gyroscope readings. The model integrates an indirect Kalman filter, and it tracks the errors in the orientation, linear acceleration and gyroscope offset. The software code used to calculate the orientation is based on [35]. The recorded linear acceleration and angular velocity and the estimated orientation of the arm of the user are shown in Fig. 5.a.

2) ELECTROMYOGRAPHY

The implemented hand gesture recognition algorithm is the same as that presented in [34]. Before starting the rehabilitation exercise, the subjects are asked to perform a calibration to determine the maximum voluntary contraction (MVC) values and two EMG threshold values. The MVC values of each muscle (MVC_{ED} and MVC_{FDS}) are computed as the maximum value of the corresponding rectified EMG signal (rEMG) during the calibration. The flexor (μ) and extensor (ε) thresholds are the maximum limit values corresponding to muscular deactivation of the FDS and ED muscles, respectively. The raw EMG signals are sampled at 200 Hz and transmitted to the TMS320F28069M MCU via i2C communication. The signals are filtered with a notch filter (50 Hz center frequency) and a high-pass filter (0.01 Hz stopband frequency and 10 Hz passband frequency) (Fig. 5.b). The filtered signals are rectified by calculating the root mean square (RMS) with a 10-point window and low-pass filtered (1 Hz passband edge frequency). The rectified signals are normalized (nEMG) with respect to their MVC.

The determination of the hand gesture depends on the instantaneous values of the nEMG signals and the thresholds. The closed hand gesture is recognized when $nEMG_{FDS}$ crosses over the flexor threshold μ while $nEMG_{FDS}$ is larger than $nEMG_{ED}$ if it exceeds ε. Similarly, the open hand gesture is recognized when $nEMG_{ED}$ crosses over the extensor threshold ε while $nEMG_{ED}$ is larger than $nEMG_{FDS}$ if it exceeds μ. The rest gesture is determined when both EMG normalized signals are lower than their respective threshold.

B. ADAPTIVE CONTROL

The second proposed rehabilitation scenario is the implementation of an AAN strategy that adjusts the level of assistance of a wrist rehabilitation robot according to the emotional state of the patient and the motor performance. The 3-DoF wrist rehabilitation robot has one encoder for each degree and a cylindrical handle with a force sensor [36] for biomechanical measurements and thus determination of the user performance.

Previous studies have shown that the HR increases as a response to physical effort, the SCL and SCR frequency increase with arousal or emotional excitement and mental workload, and the SKT decreases as a result of cognitive workload and anxiety [37]. Considering this, the application uses three different physiological signals (ECG, GSR and SKT) to estimate the user's emotional state in the two-dimensional model (arousal and valence).

A two-stage fuzzy logic approach based on [16], [22] was developed to adaptatively estimate the level of assistance considering the user emotion and motor performance (Fig. 6).

First, arousal and valence changes (increase, constant, or decrease) are determined based on the variations in the HR, SCL, SCR frequency and SKT signals normalized with respect to their resting values (previously determined in a calibration process). The motor performance is evaluated considering the biomechanical information provided by the sensors embedded in the robot: user motion and applied forces.

The second stage of the fuzzy logic approach determines whether to increase, maintain or decrease the level of assistance of the wrist rehabilitation platform considering the arousal and valence values in combination with motor performance.

The AAN paradigm is based on a robot closed-loop admittance controller [38]. The M, B, and K parameters, which characterize the admittance controller, are updated (increase, decrease, or no change) every second according to the fuzzy logic output.

GSR, ECG and SKT analyses are computed in the real-time microcontroller. Then, the extracted features (SCL, SCR, HR, and SKT) are sent via BLE to the PC. Hence, these features along with the force and motion are used to run the fuzzy logic control in the PC to estimate the level of assistance and to send the K, B, and M variables back to the robot to update the admittance controller.

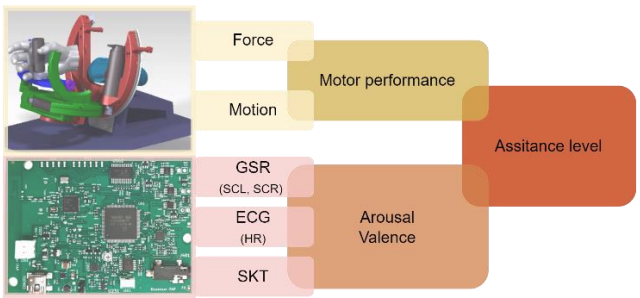

FIGURE 6. Two-stage fuzzy logic model for mapping physiological (GSR, ECG and SKT) and biomechanical (motion and force) information to the assistance level of the rehabilitation robot.

User training with the wrist rehabilitation robot is shown in Fig. 3.b. Disposable pre-gelled electrodes are attached to the user for ECG recording (two electrodes on the torso and one on the umbilical region). Additionally, two electrodes are placed at the fingertips of the index and middle fingers for GSR measurements. The IR thermometer that sits underneath the embedded platform is used for determining the SKT.

1) ELECTROCARDIOGRAM

The ECG signal is analog-to-digital converted in the TMS320F28069M with a sampling frequency of 500 Hz. The heart rate is determined from the RR intervals of the ECG signal, which are detected using the well-known real-time algorithm developed by Pan and Tompkins [39]. The processed ECG signal indicating the R events of a person at rest is shown in Fig. 7.

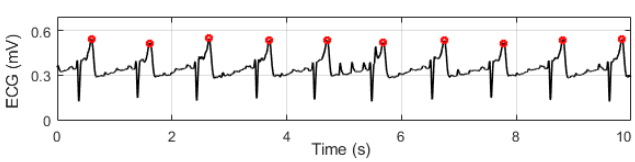

FIGURE 7. ECG signal including R events detection.

2) GALVANIC SKIN RESPONSE

The GSR signal can be split into two main components: the tonic component or SCL and phasic component or SCR. The SCL changes slightly over time and is known to be related to hydration, skin dryness and automatic regulation. It reflects general changes in autonomic arousal. The SCR shows faster changing elements of the signal and is sensitive to emotionally arousing stimulus events.

The output of the GSR module is analog-to-digital converted in the TMS320F28069M with a sampling frequency of 225 Hz. The raw SC signal is filtered (10 Hz low-pass filter) to reduce high-frequency noise and thus decrease false-positive detection of phasic events. Then, the SCL (baseline of the SC) and SCR (evoked changes in skin conductance) components are calculated based on [40], in which a deconvolution technique is implemented. The raw and filtered SC signal and its tonic and phasic components of a person under different visual stimuli are shown in Fig. 8.

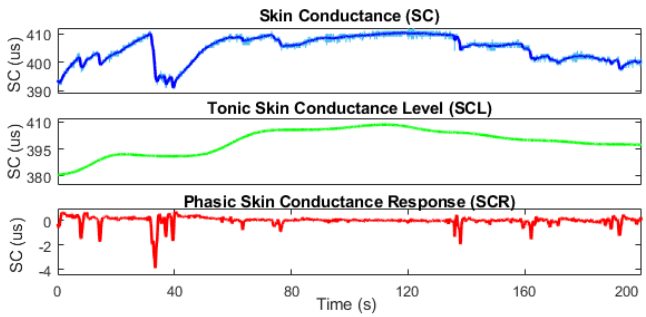

FIGURE 8. Raw and filtered SC signal, tonic skin conductance level (SCL) and phasic skin conductance response (SCR).

C. POWER CONSUMPTION

An important feature of the presented system is its computational capabilities and power consumption. As previously mentioned, the battery lasts for 5 hours with a maximum power consumption of approximately 1250 mW. In this section, the system consumption is analyzed in detail. For this, the system is divided into three main parts: sensor modules, TMS320F28069M MCU and CC2650 MCU.

The EMG, IMU, ECG, GSR and TEMP modules when active and configured with the specifications previously defined have a power consumption of 40.6 mW, 5.6 mW, 0.6 mW, 3.3 mW and 5.6 mW, respectively. On the other hand, their power consumption in sleep mode is 9.6 mW, 0.02 mW, 0.001 mW, 2.6 mW and 0.01 mW.

Furthermore, the power consumption of the TMS320F28069M microcontroller was analyzed for the two proposed scenarios. The breakdown of the average power consumption of each peripheral for each application is detailed in Fig. 9. During data acquisition from the sensors (using ADC, SPI or i2C interfaces), the DMA is triggered and used to transfer sampled data to the internal memory. The CLA module is used to carry out the signal processing independently of the main core. The DMA energy consumption depends on the number of active channels, and it is proportional to the amount of data and transfer rate, while the CLA energy consumption is proportional to the computational load, i.e., to the algorithm complexity.

The power consumption of the system is highly influenced by the application and, consequently, the MCU configuration. Additionally, the energy consumption of the microcontroller is extremely variable according to the computational load. The microcontroller can be programmed to go into an IDLE mode (main CPU is halted while peripherals and other clocks remain active) when the desired computation is over, which drastically decreases the power consumption from 272.3 mW to only 82.5 mW. Since the signal processing is mainly carried out in the CLA, the MCU spends more than 80% of its duty cycle (90 MHz) in IDLE mode. We found a 203 mW power consumption for motion recognition control and 249 mW for adaptive control.

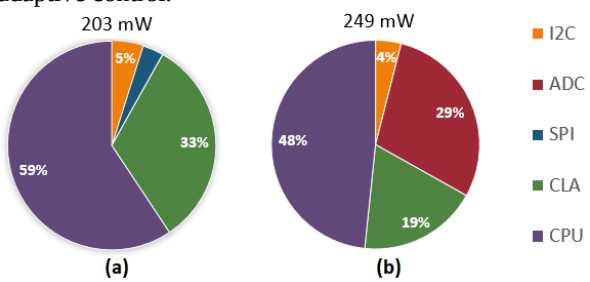

FIGURE 9. Breakdown of the microcontroller power consumption for the two proposed scenarios: (a) motion recognition control and (b) adaptive control.

The power consumption of the CC2650 module is mostly due to BLE communication. The average power consumption of the BLE communication is proportional to the amount of sent data and can reach a maximum of 32.7 mW when streaming the raw data from the five sensor modules simultaneously at 1 kHz. In the proposed scenarios, the CC2650 MCU only receives information through the i2c interface to send it to a central node using BLE. Therefore, neither additional modules nor data processing is carried out, which would increase the power consumption of this module.

IV. DISCUSSION

We have presented a low-cost wearable embedded platform for implementation of biocooperative control in the context of neuromotor rehabilitation. The compact platform is highly versatile in terms of the diversity of the sensors that it integrates (IMU, EMG, SKT, GSR, and ECG). Although some low-cost wearable platforms have been previously proposed, they did not integrate so many sensors since they were not developed with this approach. For instance, [41]–[43] only integrated EMG sensors, [44],[45] only developed an ECG sensor and [46] only used IMU sensors. [47] incorporated ECG and GSR sensors, [48] integrated IMU and ECG sensors, and [49] incorporated GSR, SKT and IMU sensors.

The selection of these five sensors is based on a review of the related literature. The detection of motion based on data collected from IMUs has been widely used for rehabilitation purposes. In [50]–[55], a wireless IMU was used for stroke rehabilitation in combination with or without motion-sensitive games based on VR (IMU-based exergames). IMU information has also been used for biomechanical analysis [56]–[60], such as gait analysis, which can be used to evaluate motor recovery. It can also be used with assistive devices [61]–[64] and in combination with other sensors, such as EMG sensors [5], [7]. Features extracted from EMG signals have been used as inputs of the control loop of rehabilitation robots [65]–[68]. EMG has also been used to identify fatigue during rehabilitation [13], [69] and even emotional states [17], [19]–[21]. Although there is no consensus as to which physiological signals are the best to use to determine the psychophysiological state, measurements of the SCR frequency, SCL, HR and SKT can give reliable information about the psychophysiological state of the patient [36], [70].

The presented system is open and configurable so that researchers can easily develop new biocooperative control strategies as well as modify and optimize existing algorithms. The high-efficiency real-time microcontroller provides high processing capabilities for implementing this kind of biocooperative control, which requires complex signal processing. Additionally, its high flexibility regarding the diversity of sensors and wireless communication allows the development of a multitude of rehabilitation applications.

Two possible applications have been proposed. The applications use different signals, and the training approaches are different; while the first one does not require an assistive robotic device and uses EMG and IMU information, the second one needs an assistive robot and uses GSR, ECG and SKT data. It has been verified that even though the system is low cost, the quality of the acquired signals is reliable for implementing biocooperative control algorithms. Raw and processed data from all sensors have been shown: motion has been identified using IMU measurements, hand gestures have been recognized using EMG signals, the HR has been detected from ECG signals, the SCL and SCR have been acquired from recorded GSR data and the SKT has been continuously monitored.

Additionally, the power consumption of the system has been carefully analyzed for the two scenarios, which are fully compliant with the energy constraints of the wearable system. Furthermore, the high-efficiency processing capabilities of the platform have been tested. This platform supports the real-time execution of more complex algorithms than those presented for the two rehabilitation scenarios.

In summary, an embedded platform for implementing real-time biocooperative control in the context of neurorehabilitation has been presented. The open and highly customizable system is more convenient for developers than proprietary solutions; it can be used for any purposes (from only physiological signal acquisition for later offline analysis to implementation of complex biocooperative control) since researchers can freely modify the program and add new features and capabilities without any restrictions. The platform includes a high diversity of sensors and wireless communication while being low cost, compact, and

comfortable to wear. For these reasons, the quality level of its signals will never reach that of the signals recorded by commercial acquisition systems. On the other hand, it has been verified that the quality of the signals is reliable enough for the two proposed scenarios, and therefore, good performance is expected in other related applications.

The design of the presented wearable system was based on a trade-off between complexity, price, and performance: volume, flexibility, energy consumption, onboard processing, signal quality, etc. The final solution can record and process real-time multimodal information with a decent quality for at least 5 hours. However, it is not suitable for applications that require a high signal quality or a long-term life battery, but these requirements are not expected in most of the potential applications related to neurorehabilitation.

V. CONCLUSION

The presented platform is low-cost, wearable, customizable and open for implementing real-time biocooperative control. The high versatility of the system along with the high-efficiency real-time microcontrollers will enable researchers to translate biocooperative control strategies that rely on physiological signals into affordable real-word solutions. Furthermore, the quality of the recorded signals meets the needs of two common use cases in the context of upper-limb neuromotor rehabilitation. The accessibility of this technology may promote research and development of biocooperative control since one of the main limitations is the high cost of the necessary signal acquisition systems.

REFERENCES

[1] R. Riener, A. Koenig, M. Bolliger, M. Wieser, A. Duschau-Wicke, and H. Vallery, "Bio-cooperative robotics: Controlling mechanical, physiological and mental patient states," 2009 IEEE Int. Conf. Rehabil. Robot. ICORR 2009, pp. 407–412, 2009.

[2] R. Riener and M. Munih, "Guest editorial special section on rehabilitation via bio-cooperative control," IEEE Trans. Neural Syst. Rehabil. Eng., vol. 18, no. 4, pp. 337–338, 2010.

[3] N. Garcia-aracil, C. Perez-vidal, J. M. Sabater, and E. Papaleo, "Patient-Tailored Assistance. A new Concept of Assistive Robotic Devices That Adapts to Individual Users," IEEE Robotics, pp. 123–133, 2014.

[4] J. Zhang, B. Wang, C. Zhang, Y. Xiao, and M. Y. Wang, "An EEG/EMG/EOG-based multimodal human-machine interface to real-time control of a soft robot hand," Front. Neurorobot., vol. 13, no. March, 2019.

[5] A. Krasoulis, S. Vijayakumar, and K. Nazarpour, "Multi-grip classification-based prosthesis control with two EMG-IMU sensors," bioRxiv, vol. 28, no. 2, pp. 508–518, 2019.

[6] M. Landgraf et al., "Gesture Recognition with Sensor Data Fusion of Two Complementary Sensing Methods *," 2018.

[7] A. Fougner, E. Scheme, A. D. C. Chan, K. Englehart, and Ø. Stavdahl, "Resolving the limb position effect in myoelectric pattern recognition," IEEE Trans. Neural Syst. Rehabil. Eng., vol. 19, no. 6, pp. 644–651, 2011

[8] G. Chen et al., "Adaptive control strategy for gait rehabilitation robot to assist-when-needed," 2018 IEEE Int. Conf. Real-Time Comput. Robot. RCAR 2018, pp. 538–543, 2019.

[9] J. C. Fraile et al., "E2Rebot: A robotic platform for upper limb rehabilitation in patients with neuromotor disability," Adv. Mech. Eng., vol. 8, no. 8, pp. 1–13, 2016.

[10] T. Teramae, T. Noda, and J. Morimoto, "EMG-Based Model Predictive Control for Physical Human-Robot Interaction: Application for Assist-As-Needed Control," IEEE Robot. Autom. Lett., vol. 3, no. 1, pp. 210–217, 2018.

[11] K. Gui, U.-X. Tan, H. Liu, and D. Zhang, "Electromyography-Driven Progressive Assist-as-Needed Control for Lower Limb Exoskeleton," IEEE Trans. Med. Robot. Bionics, vol. 2, no. 1, pp. 50–58, 2020.

[12] A. Cisnal, R. Alonso, J. P. Turiel, J. C. Fraile, V. Lobo, and V. Moreno, "EMG Based Bio-Cooperative Direct Force Control of an Exoskeleton for Hand Rehabilitation: A Preliminary Study," in ICNR BIOSYSROB, 2019, vol. 21, pp. 390–394.

[13] F. Scotto Di Luzio et al., "Bio-cooperative approach for the human-in-the-loop control of an end-effector rehabilitation robot," Front. Neurorobot., vol. 12, no. October, pp. 1–12, 2018.

[14] D. Novak, M. Mihelj, J. Ziherl, A. Olenšek, and M. Munih, "Psychophysiological measurements in a biocooperative feedback loop for upper extremity rehabilitation," IEEE Trans. Neural Syst. Rehabil. Eng., vol. 19, no. 4, pp. 400–410, 2011.

[15] M. Mihelj, D. Novak, and M. Munih, "Emotion-aware system for upper extremity rehabilitation," 2009 Virtual Rehabil. Int. Conf. VR 2009, pp. 160–165, 2009.

[16] C. R. Guerrero, J. C. Fraile Marinero, J. P. Turiel, and V. Muñoz, "Using 'human state aware' robots to enhance physical human-robot interaction in a cooperative scenario," Comput. Methods Programs Biomed., vol. 112, no. 2, pp. 250–259, 2013.

[17] E. Gümüslü, D. Erol Barkana, and H. Köse, "Emotion recognition using EEG and physiological data for robot-assisted rehabilitation systems," ICMI 2020 Companion - Companion Publ. 2020 Int. Conf. Multimodal Interact., pp. 379–387, 2020.

[18] M. Khezri, M. Firoozabadi, and A. R. Sharafat, "Reliable emotion recognition system based on dynamic adaptive fusion of forehead biopotentials and physiological signals," Comput. Methods Programs Biomed., vol. 122, no. 2, pp. 149–164, 2015.

[19] A. Hariharan and M. T. P. Adam, "Blended Emotion Detection for Decision Support," IEEE Trans. Human-Machine Syst., vol. 45, no. 4, pp. 510–517, 2015.

[20] S. Koelstra et al., "DEAP: A database for emotion analysis; Using physiological signals," IEEE Trans. Affect. Comput., vol. 3, no. 1, pp. 18–31, 2012.

[21] J. Kim and E. André, "Emotion recognition based on physiological changes in music listening," IEEE Trans. Pattern Anal. Mach. Intell., vol. 30, no. 12, pp. 2067–2083, 2008.

[22] R. L. Mandryk and M. S. Atkins, "A fuzzy physiological approach for continuously modeling emotion during interaction with play technologies," Int. J. Hum. Comput. Stud., vol. 65, no. 4, pp. 329–347, 2007.

[23] C. Liu, K. Conn, N. Sarkar, and W. Stone, "Physiology-based affect recognition for computer-assisted intervention of children with Autism Spectrum Disorder," Int. J. Hum. Comput. Stud., vol. 66, no. 9, pp. 662–677, 2008.

[24] R. W. Picard, E. Vyzas, and J. Healey, "Toward machine emotional intelligence: Analysis of affective physiological state," IEEE Trans. Pattern Anal. Mach. Intell., vol. 23, no. 10, pp. 1175–1191, 2001.

[25] J. Zhai, A. B. Barreto, C. Chin, and C. Li, "Realization of stress detection using psychophysiological signals for improvement of human-computer interactions," in IEEE, 2005, pp. 415–420.
[26] F. J. Badesa, R. Morales, N. Garcia-Aracil, J. M. Sabater, A. Casals, and L. Zollo, "Auto-adaptive robot-aided therapy using machine learning techniques," Comput. Methods Programs Biomed., vol. 116, no. 2, pp. 123–130, 2014.
[27] D. Novak and R. Riener, "A survey of sensor fusion methods in wearable robotics," Rob. Auton. Syst., vol. 73, pp. 155–170, 2015.
[28] I. Herrera-Luna, E. J. Rechy-Ramirez, H. V. Rios-Figueroa, and A. Marin-Hernandez, "Sensor Fusion Used in Applications for Hand Rehabilitation: A Systematic Review," IEEE Sens. J., vol. 19, no. 10, pp. 3581–3592, 2019.
[29] B. Jakopin, M. Mihelj, and M. Munih, "An Unobtrusive Measurement Method for Assessing Physiological Response in Physical Human-Robot Interaction," IEEE Trans. Human-Machine Syst., vol. 47, no. 4, pp. 474–485, 2017.
[30] O. Postolache, V. Viegas, J. M. Dias Pereira, D. Vinhas, P. S. Girão, and G. Postolache, "Toward developing a smart wheelchair for user physiological stress and physical activity monitoring," IEEE MeMeA 2014 - IEEE Int. Symp. Med. Meas. Appl. Proc., 2014.
[31] S. Heuer, B. Chamadiya, A. Gharbi, C. Kunze, and M. Wagner, "Unobtrusive in-vehicle biosignal instrumentation for advanced driver assistance and active safety," Proc. 2010 IEEE EMBS Conf. Biomed. Eng. Sci. IECBES 2010, no. December, pp. 252–256, 2010.
[32] A. I. Faisal, S. Majumder, R. Scott, T. Mondal, D. Cowan, and M. Jamal Deen, "A Simple, Low-Cost Multi-Sensor-Based Smart Wearable Knee Monitoring System," IEEE Sens. J., vol. 21, no. 6, pp. 8253–8266, 2021.
[33] S. Qiu *et al.*, "Multi-sensor information fusion based on machine learning for real applications in human activity recognition: State-of-the-art and research challenges," *Information Fusion*, vol. 80. Elsevier B.V., pp. 241–265, Apr. 01, 2022. doi: 10.1016/j.inffus.2021.11.006.
[34] A. Cisnal, J. Perez-Turiel, J. C. Fraile, D. Sierra, and E. De La Fuente, "RobHand: A Hand Exoskeleton with Real-Time EMG-Driven Embedded Control. Quantifying Hand Gesture Recognition Delays for Bilateral Rehabilitation," IEEE Access, vol. 9, pp. 137809–137823, 2021.
[35] "Open Source Sensor Fusion". [Online]. Available: https://github.com/memsindustrygroup/Open-Source-Sensor-Fusion.
[36] A. Cisnal, V. Martínez-Cagigal, G. Alonso-Linaje, S. Moreno-Calderón, J. Pérez-Turiel, R. Hornero and J.C. Fraile, "An Overview of M3Rob, a Robotic Platform for Neuromotor and Cognitive Rehabilitation Using Augmented Reality," in XL Congreso Annual de la Sociedad Española de Ingeniería Biomédica, Nov. 2022, pp. 180-183, ISBN 978-84-09-45972-8
[37] D. Novak et al., "Psychophysiological responses to robotic rehabilitation tasks in stroke," IEEE Trans. Neural Syst. Rehabil. Eng., vol. 18, no. 4, pp. 351–361, 2010.
[38] C. D. R. Guerrero, J. C. F. Marinero, and J. P. Turiel, "Robot adaptive behavior to suit patient needs and enable more intensive rehabilitation tasks," IEEE 2009 Int. Conf. Mechatronics, ICM 2009, no. April, 2009.
[39] J. Pan and W. J. Tompkins, "A Real-Time QRS Detection Algorithm," IEEE Trans. Biomed. Eng., vol. BME-32, no. 3, pp. 230–236, 1985.
[40] J. E. Muñoz, E. R. Gouveia, M. S. Cameirão, and S. B. I. Badia, "Physiolab - A multivariate physiological computing toolbox for ECG, EMG and EDA signals: A case of study of cardiorespiratory fitness assessment in the elderly population," Multimed. Tools Appl., vol. 77, no. 9, pp. 11511–11546, 2018.
[41] S. Benatti et al., "A Versatile Embedded Platform for EMG Acquisition and Gesture Recognition," IEEE Trans. Biomed. Circuits Syst., vol. 9, no. 5, pp. 620–630, 2015.
[42] S. Örücü and M. Selek, "Design and Validation of Multichannel Wireless Wearable SEMG System for Real-Time Training Performance Monitoring," J. Healthc. Eng., vol. 2019, pp. 1–15, 2019.
[43] D. Brunelli, E. Farella, D. Giovanelli, B. Milosevic, and I. Minakov, "Design considerations for wireless acquisition of multichannel sEMG signals in prosthetic hand control," IEEE Sens. J., vol. 16, no. 23, pp. 8338–8347, 2016
[44] C. Athavipach, S. Pan-Ngum, and P. Israsena, "A wearable in-ear EEG device for emotion monitoring," *Sensors (Switzerland)*, vol. 19, no. 18, Sep. 2019, doi: 10.3390/s19184014.
[45] A. Nguyen *et al.*, "LIBS: A Lightweight and Inexpensive In-Ear Sensing System for Automatic Whole-Night Sleep Stage Monitoring," *GetMobile: Mobile Comp. and Comm.*, vol. 21, no. 3, pp. 31–34, 2017, doi: 10.1145/3161587.3161596.
[46] G. Marta *et al.*, "Wearable Biofeedback Suit to Promote and Monitor Aquatic Exercises: A Feasibility Study," *IEEE Trans Instrum Meas*, vol. 69, no. 4, pp. 1219–1231, Apr. 2020, doi: 10.1109/TIM.2019.2911756.
[47] B. F. Villar, A. C. de la Rica, M. M. Vargas, J. P. Turiel, and M. Juan Carlos Fraile, "A low Cost IoT enabled device for the monitoring, recording and communication of physiological signals," BIODEVICES 2021 - 14th Int. Conf. Biomed. Electron. Devices; Part 14th Int. Jt. Conf. Biomed. Eng. Syst. Technol. BIOSTEC 2021, vol. 1, no. Biostec, pp. 135–143, 2021.
[48] Y. D'Mello et al., "Real-time cardiac beat detection and heart rate monitoring from combined seismocardiography and gyrocardiography," Sensors (Switzerland), vol. 19, no. 16, 2019.
[49] J. Huan et al., "A Wearable Skin Temperature Monitoring System for Early Detection of Infections," IEEE Sens. J., vol. 22, no. 2, pp. 1670–1679, 2022.
[50] K. Kadir, Z. M. Yusof, M. Z. M. Rasin, M. M. Billah, and Q. Salikin, "Wireless IMU: A Wearable Smart Sensor for Disability Rehabilitation Training," 2018 2nd Int. Conf. Smart Sensors Appl. ICSSA 2018, pp. 53–57, 2018.
[51] Z. X. Yin and H. M. Xu, "A wearable rehabilitation game controller using IMU sensor," Proc. 4th IEEE Int. Conf. Appl. Syst. Innov. 2018, ICASI 2018, pp. 1060–1062, 2018.
[52] A. Romano et al., "Upper Body Physical Rehabilitation for Children with Ataxia through IMU-Based Exergame," J. Clin. Med., vol. 11, no. 4, 2022.
[53] M. Lapresa et al., "A Smart Solution for Proprioceptive Rehabilitation through M-IMU Sensors," 2020 IEEE Int. Work. Metrol. Ind. 4.0 IoT, MetroInd 4.0 IoT 2020 - Proc., pp. 591–595, 2020.
[54] C. J. Chen, Y. T. Lin, C. C. Lin, Y. C. Chen, Y. J. Lee, and C. Y. Wang, "Rehabilitation System for Limbs using IMUs," Proc. - Int. Symp. Qual. Electron. Des. ISQED, vol. 2020-March, pp. 285–291, 2020.
[55] M. Kim, J. Cho, S. Lee, and Y. Jung, "Imu sensor-based hand gesture recognition for human-machine interfaces," Sensors (Switzerland), vol. 19, no. 18, pp. 1–13, 2019.
[56] J. W. Seo and H. S. Kim, "Biomechanical analysis in five bar linkage prototype machine of gait training and rehabilitation by imu sensor and electromyography," Sensors, vol. 21, no. 5, pp. 1–10, 2021.
[57] M. Mundt et al., "Estimation of Gait Mechanics Based on Simulated and Measured IMU Data Using an Artificial Neural Network," Front. Bioeng. Biotechnol., vol. 8, no. February, pp. 1–16, 2020.

[58] H. Lim, B. Kim, and S. Park, "Prediction of lower limb kinetics and kinematics during walking by a single IMU on the lower back using machine learning," Sensors (Switzerland), vol. 20, no. 1, 2020.
[59] D. Stanev, D. Tsaopoulos, and K. Moustakas, "Using Marker- and IMU-Based Solutions in Rehabilitation," Sensors, vol. 21, no. 1804, pp. 1–20, 2021.
[60] A. Talitckii *et al.*, "Comparative Study of Wearable Sensors, Video, and Handwriting to Detect Parkinson's Disease," *IEEE Trans Instrum Meas*, vol. 71, 2022, doi: 10.1109/TIM.2022.3176898.
[61] K. Little et al., "IMU-based assistance modulation in upper limb soft wearable exosuits," IEEE Int. Conf. Rehabil. Robot., vol. 2019-June, pp. 1197–1202, 2019.
[62] D. A. Bennett and M. Goldfarb, "IMU-Based Wrist Rotation Control of a Transradial Myoelectric Prosthesis," IEEE Trans. Neural Syst. Rehabil. Eng., vol. 26, no. 2, pp. 419–427, 2018.
[63] S. Yu et al., "Design and Control of a Quasi-Direct Drive Soft Exoskeleton for Knee Injury Prevention during Squatting," arXiv, vol. 4, no. 4, pp. 4579–4586, 2019.
[64] C. Shi, L. Qi, D. Yang, J. Zhao, and H. Liu, "A novel method of combining computer vision, eye-tracking, EMG, and IMU to control dexterous prosthetic hand," IEEE Int. Conf. Robot. Biomimetics, ROBIO 2019, no. December, pp. 2614–2618, 2019.
[65] N. Lotti et al., "Myoelectric or Force Control? A Comparative Study on a Soft Arm Exosuit," IEEE Trans. Robot., vol. 38, no. 3, pp. 1363–1379, 2022.
[66] F. Missiroli, N. Lotti, M. Xiloyannis, L. H. Sloot, R. Riener, and L. Masia, "Relationship Between Muscular Activity and Assistance Magnitude for a Myoelectric Model Based Controlled Exosuit," Front. Robot. AI, vol. 7, no. December, pp. 1–13, 2020.
[67] S. Yao, Y. Zhuang, Z. Li, and R. Song, "Adaptive admittance control for an ankle exoskeleton using an EMG-driven musculoskeletal model," Front. Neurorobot., vol. 12, no. APR, 2018.
[68] A. Cisnal, D. Sierra, J. P. Turiel, and J. C. Fraile, "An embedded implementation of EMG-driven control for assisted bilateral therapy," in Converging Clinical and Engineering Research on Neurorehabilitation IV. ICNR 2020. Biosystems & Biorobotics, D. Torricelli, M. Akay, and J. L. Pons, Eds. Springer, 2020, pp. 817–821.
[69] H. Xu and A. Xiong, "Advances and disturbances in sEMG-Based intentions and movements recognition: A review," IEEE Sens. J., vol. 21, no. 12, pp. 13019–13028, 2021.
[70] C. Rodriguez Guerrero, J. Fraile Marinero, J. Perez Turiel, and P. Rivera Farina, "Bio cooperative robotic platform for motor function recovery of the upper limb after stroke," 2010 Annu. Int. Conf. IEEE Eng. Med. Biol. Soc. EMBC'10, pp. 4472–4475, 2010.

ANA CISNAL (S'18) became a Student Member in 2018. She received a B.S. degree in industrial electronics and automation engineering and an M.S. degree in industrial engineering from the University of Valladolid, Spain, in 2017 and 2019, respectively. She is currently pursuing a Ph.D. degree in industrial engineering at the University of Valladolid.

During 2016, she participated in quality internships at the Technology Center CARTIF (Valladolid, Spain) and Fraunhofer IBMT (Sankt Ingbert, Germany). From 2017 until now, she has been working at the Advanced Production Technologies Institute (ITAP) of the University of Valladolid as a research fellowship and a contract researcher. Her current line of research is the development of control strategies for biocooperative controls for robotic neuromotor rehabilitation platforms.

DANIEL ANTOLÍNEZ received a B.S. degree in industrial electronics and automation engineering from the University of Valladolid, Valladolid, Spain, in 2021. He is currently pursuing an M.S degree in research of information and communications technologies (ICT at the University of Valladolid. During 2019, he had an internship at the Technology Center CARTIF.

Since 2021, he has been working at the Institute of Advanced Production Technologies (ITAP), Valladolid University, as a Research Fellow. His current research interest is in the electronic design of printed circuit boards, focused mainly on biomedical applications.

JAVIER P. TURIEL is an Associate Professor at the Department of Systems Engineering of the University of Valladolid (Spain), from which he received a Ph.D. degree in Control Engineering in 1994. In 1999, he was a visiting professor at the Electrical Engineering and Computer Science Dpt. (EECS), University of Michigan (US).

He was the Head of the Biomedical engineering division at CARTIF Technological Centre from 2000 to 2014. He is also a member of the Medical Robotics group at the ITAP (Institute of Advanced Production Technologies) University Institute. His research interests include surgical and rehabilitation robots.

JUAN CARLOS FRAILE received a Ph.D. degree in control engineering from the Faculty of engineering, University of Valladolid, Spain, in 1987. Since 1992, he has been an Associate Professor of control and robotics in the Faculty of Engineering, University of Valladolid. In 1998, he held a visiting professor position at ICES, Institute of Complex Engineering Systems, Engineering Systems, Carnegie Mellon University, Pittsburgh, USA. He is the leader of the ITAP-Medical Robotics group at the University of Valladolid. His current research interests include rehabilitation robotics and robots for surgery.

EUSEBIO DE LA FUENTE received an M.Sc. degree in electronic engineering and automatic control and a Ph.D. degree from the University of Valladolid, Spain, in 1991 and 1997, respectively.

Since 1999, he has been an Associate Professor in computer science with a specialization in computer vision at the Industrial Engineering School, Valladolid, Spain. His current research interests include the field of medical image processing and real-time video analysis for rehabilitation and surgical robot applications. He is especially interested in deep learning techniques for object detection in medical images and classification.